

## A SPACE QUALIFIED THERMAL IMAGING SYSTEM USING A Pt Si DETECTOR ARRAY

ROBERT W. ASTHEIMER  
EDO CORPORATION  
BARNES ENGINEERING DIVISION

### 1.0 INTRODUCTION

EDO Corporation, Barnes Engineering Division has designed and constructed a high resolution thermal imaging system on contract to Lockheed for use in the SDI Star Lab. This employs a Pt Si CCD array which is sensitive in the spectral range of 3 - 5 microns. Star Lab will be flown in the shuttle bay and consists basically of a large, reflecting, tracking telescope with associated sensors and electronics. The thermal imaging system is designed to operate in the focal plane of this telescope.

The configuration of the system is shown in Figures 1 and 2. The telescope provides a collimated beam output which is focussed onto the detector array by a silicon objective lens. The detector array subtends a field of view of  $1.6^{\circ} \times 1.22^{\circ}$ . A beam switching mirror permits bypassing the large telescope to give a field of  $4^{\circ} \times 3^{\circ}$ . Two 8 position filter wheels are provided, and background radiation is minimized by Narcissus mirrors. The detector is cooled with a Joule-Thompson cryostat fed from a high pressure supply tank. This was selected instead of a more convenient closed-cycle system because of concern with vibration; The latter may couple into the extremely critical Starlab tracking telescope.

The electronics produce a digitized video signal for recording. Offset and responsivity correction factors are stored for all pixels and these corrections are made to the digitized output in real time.

## A Space Qualified Pt Si Thermal Imaging System

This system has been evaluated as a thermal imager using a simplified optical system consisting of a 2" diameter germanium lens of 3.5" focal length. This configuration is well adapted for thermal imaging and non contact temperature measurements in space experiments such as zero gravity processing. This is the type of application addressed in this paper.

### 2.0 DETECTOR ARRAY

Platinum silicide infrared detectors are Schottky-barrier type diodes formed by the deposition of Pt Si on a silicon substrate. The incident radiation is transmitted through the silicon and absorbed in the silicide layer. Such detectors are particularly adaptable to the formation of two-dimensional arrays since, having a silicon substrate, they can be combined monolithically with a charge-coupled device (CCD) structure for reading out the signal on each detector element.

Typical spectral response of a Pt Si detector element is shown in Figure 3. It has useful response out to 5 microns, although the quantum efficiency is only about 1% at this wavelength. The silicon substrate must be shared with the CCD read out, which requires considerable space between elements in the array. The ratio of the active detector area to the total pixel area is 39%. This fill factor loss and the low quantum efficiency at longer wavelengths makes the effective  $D^*$  of a single element considerably lower than other cooled detectors used for this spectral region such as InSb. However, this is compensated by the fact that each element views the scene during the entire frame time and builds up charge which is read out at the end. This makes its imaging performance competitive with a single element InSb scanning system.

## A Space Qualified Pt Si Thermal Imaging System

The short wavelength response of the Pt Si array can be used advantageously to provide an optional near-infrared reflected image. The target would be illuminated with an incandescent lamp which will give ample radiation in the 1.2 - 2.5 micron region. The short wavelength response of the array is limited to 1.2 microns by the silicon substrate, while the glass envelope of the lamp will cut out wavelengths beyond 2.5 microns. The display could be rapidly changed from the near infrared reflected image to a thermal image by switching filters in front of the array from glass to a 2.5 micron long pass filter.

### 3.0 IMAGE COMPENSATION

In order to accurately measure radiance or temperature with a Pt Si array, three corrections must be made for variations in dark current, background radiance and responsivity between pixels. Dark current arises from thermally generated charge carriers and is dependent upon detector temperature. Back-ground is the radiance impinging on the detector elements from sources other than the desired image. This is primarily radiation from the optics and internal baffles, and is dependent upon ambient temperature. Both the dark current and background signal are unaffected by target signal strength and are, therefore, subtracted from the signal. Lastly, there are small variations in the responsivity of individual detector elements and this correction must multiply the target signal.

## A Space Qualified Pt Si Thermal Imaging System

These corrections are different for each pixel and are made in real time from three stored arrays of correction factors through the algorithm shown in Figure 4. The dark current array D is measured and stored when a liquid nitrogen cooled plate is placed in front of the detector array, while the background array B is stored when the cooled plate is placed in front of the telescope. The responsivity array is stored when viewing a uniform temperature field producing a signal about midway in the dynamic range of the detectors.

The dark current correction is adaptively adjusted for detector temperature through a single multiplier  $K_1$  which is controlled by the detector temperature. The same multiplier ( $K_1$ ) is applied to all correction terms in the array. Similarly, the background correction array is adaptively adjusted for the temperature of the optics through the single multiplier  $K_2$ .

The Starlab system is designed to measure the radiation from small targets against a space background and, under these conditions, the dark current and background compensation is essential. A saturation signal on the detector produces 4095 counts from the A/D converter. On this scale, the dark current is about 200 counts and the background 300 counts. The responsivity variation is 1% - 2%, which could be up to 80 counts. Thus we see that, even when used with a room temperature back-ground, all three compensation factors are necessary to make accurate absolute radiance or temperature measurements.

## A Space Qualified Pt Si Thermal Imaging System

The variation in dark current of a typical element with detector temperature is shown in Figure 5. If the detector temperature can be well controlled at LN<sub>2</sub> temperature (77°K), the adaptive temperature factor  $K_1$  can be eliminated. Also if the ambient temperature does not change much, the factor  $K_2$  need not be adaptive. In this case, the D and B arrays can be combined into a single non-adaptive OFFSET compensation array. This is probably adequate for shuttle experiments and would simplify the system.

### 4.0 IMAGER PERFORMANCE

The Starlab detector/electronics were preliminarily evaluated as a thermal imager by substituting a simple germanium lens for the Starlab optics. A photograph of this system is shown in Figure 6, and the major parameters are listed in Figure 7.

Figures 8 to 10 show typical false color images of near ambient objects. Unfortunately, the adaptive offset and responsivity compensation features, although operating electronically, were not yet incorporated in the system at the time these photos were made. Figure 8 shows warm water being poured from a beaker, while Figure 9 shows the same warm water being poured over a person's hand. Figure 10 shows a printed circuit board with several hot components.

A unique feature of these images, which is not evident in the photographs is that, when viewed on the TV screen, there is almost no discernable noise on any individual pixel. However in a temperature (or radiance) measuring imaging system, the performance is determined by how accurately the temperature of any

## A Space Qualified Pt Si Thermal Imaging System

element in the picture can be determined. Responsivity and offset variations between pixels produce differences in the apparent temperature of objects which must be considered as "noise", which is why, in Figure 7, we list the NET as  $0.5^\circ$  at  $110^\circ\text{C}$  without compensation. However with compensation, this will be greatly reduced and, although tests have not been completed at this date, the NET with compensation is expected to be less than  $0.02^\circ$  at  $100^\circ\text{C}$ .

A complete engineering model using flight optics and fully compensated will be tested by February 15, 1989 and the flight system will be tested in April 1989.

The Pt Si spectral response makes this detector particularly attractive for the non-contact measurement of small variations in temperature of moderately hot targets in the range of  $80+^\circ\text{C}$ . The rising responsivity at shorter wavelengths greatly enhances temperature contrast and suppresses emissivity errors.

### 5.0 CONCLUSIONS

This Pt Si CCD camera system is well suited for microgravity experiments in space, requiring accurate radiance and temperature measurements in the 3 - 5 micron region. It is very compact and directly compatible with TV. Cooling can be accomplished with a J-T cryostat as in the Starlab system or preferably with a Stirling closed-cycle cooler. The increasing detector response at short wavelengths enhances thermal contrast and enables one system to act as both a thermal and reflectively illuminated TV. Arrays with higher resolution are being developed and units with  $512 \times 512$  pixels are now available.

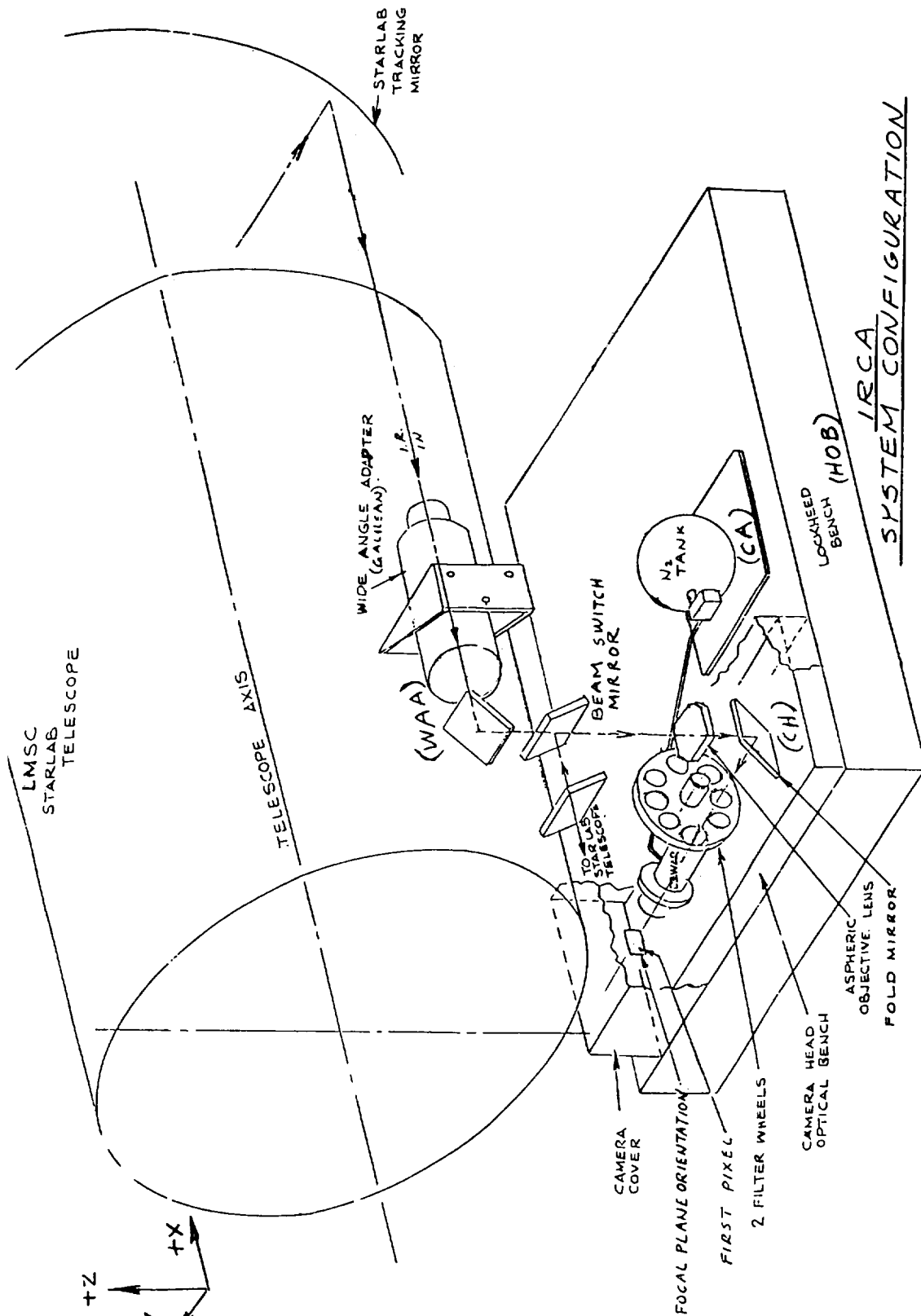
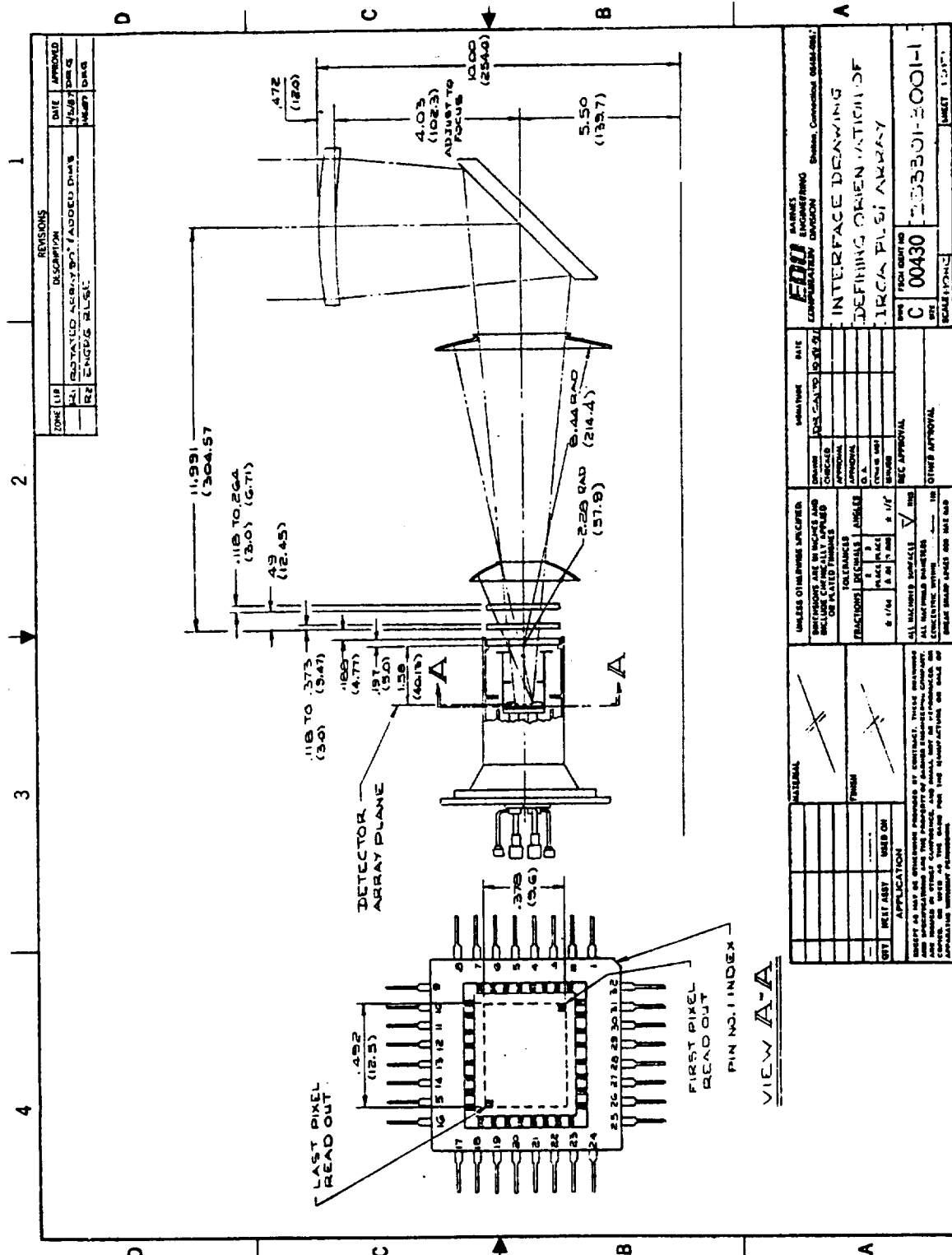


Figure 1.





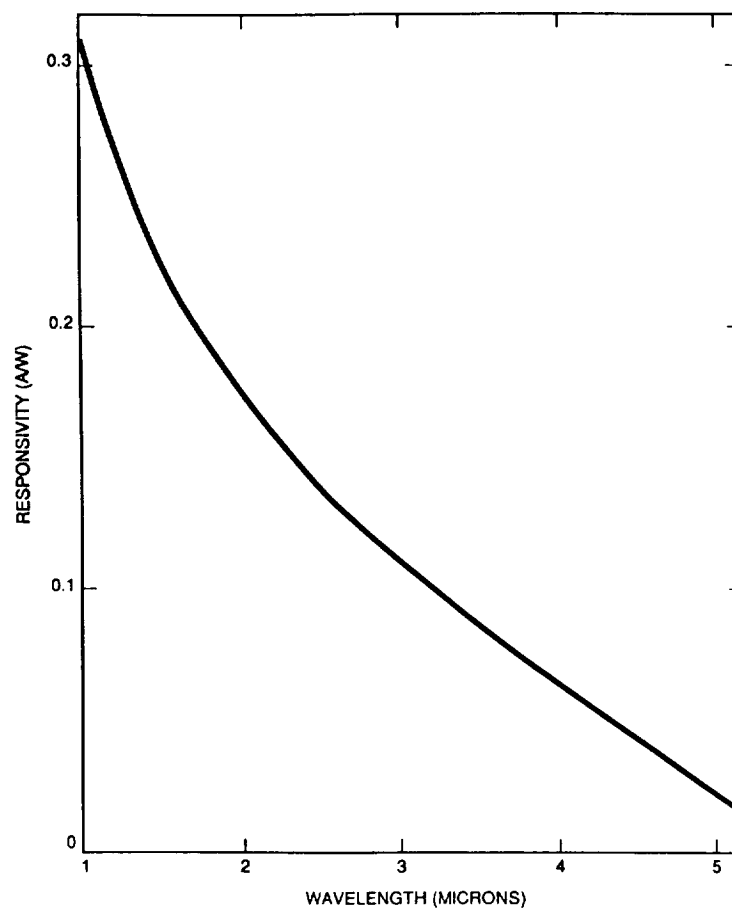


Figure 3.

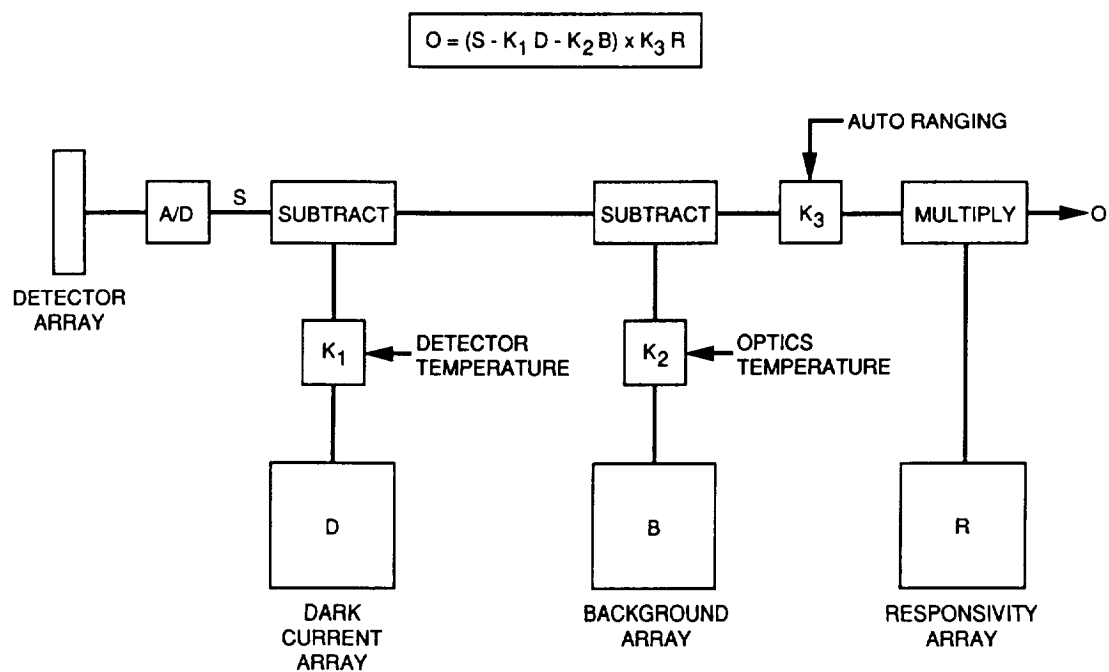


Figure 4.

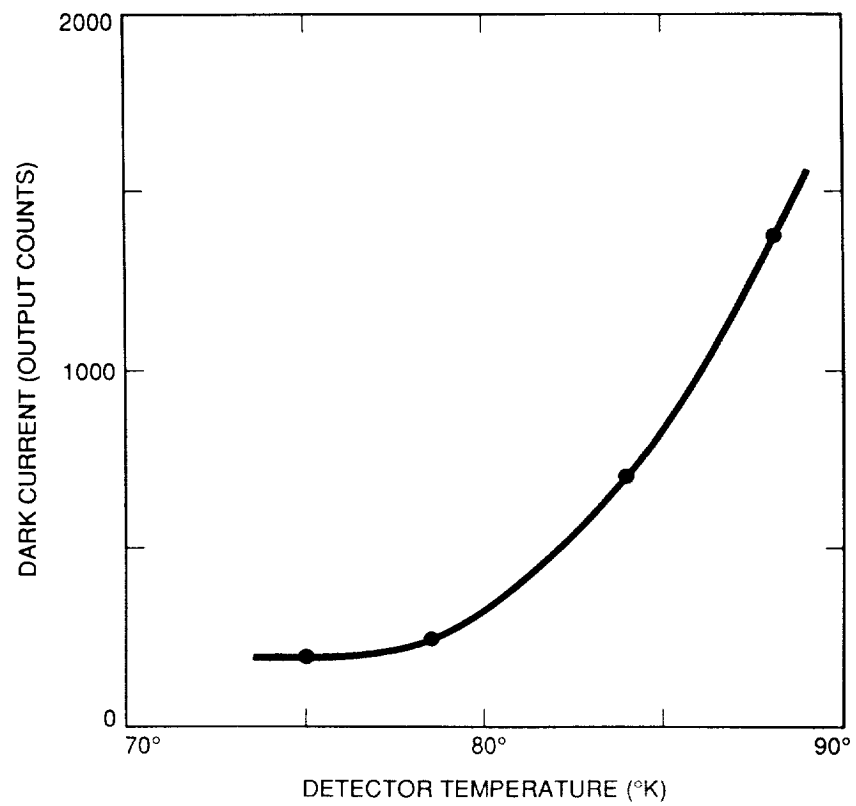


Figure 5.

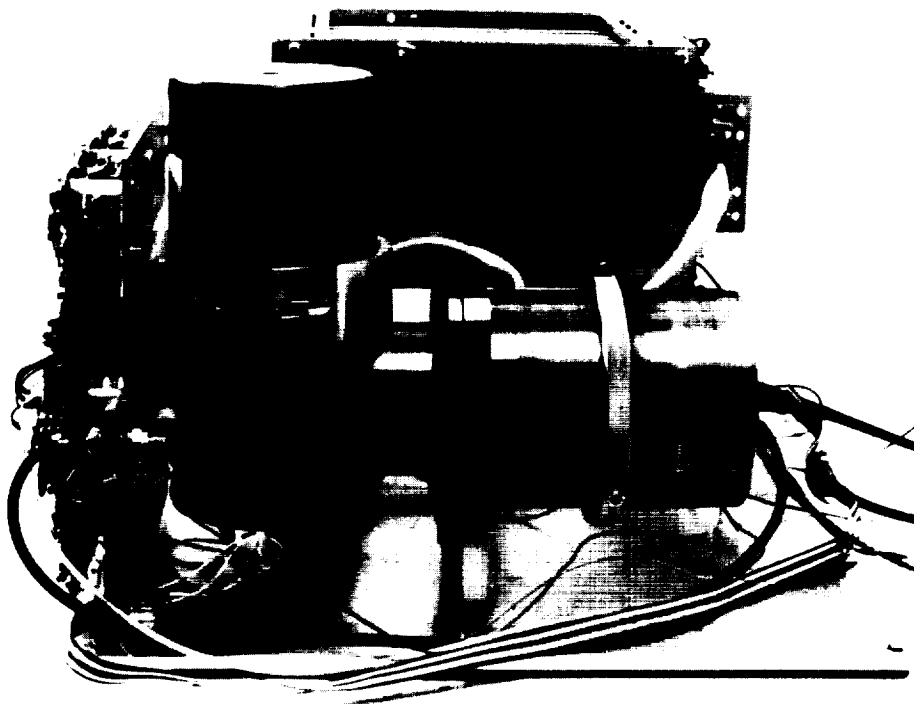


Figure 6.

## THERMAL IMAGING SYSTEM

OBJECTIVE LENS	GERMANIUM 2" DIAMETER 3.5" FOCAL LENGTH
P <sub>T</sub> S <sub>I</sub> ARRAY	160 x 244 ELEMENTS PIXEL SIZE    0.080 x 0.040 FILL FACTOR    39% TOTAL AREA    12.8 x 9.8 MM
FIELD OF VIEW	8.2° x 6.3°
PIXEL FIELD	0.9 x 0.45 MRAD
NET	0.5°C AT 100°C PATTERN NOISE LIMITED  <0.02°C AT 100°C WITH COMPENSATION

Figure 7.

ORIGINAL PAGE  
BLACK AND WHITE PHOTOGRAPH

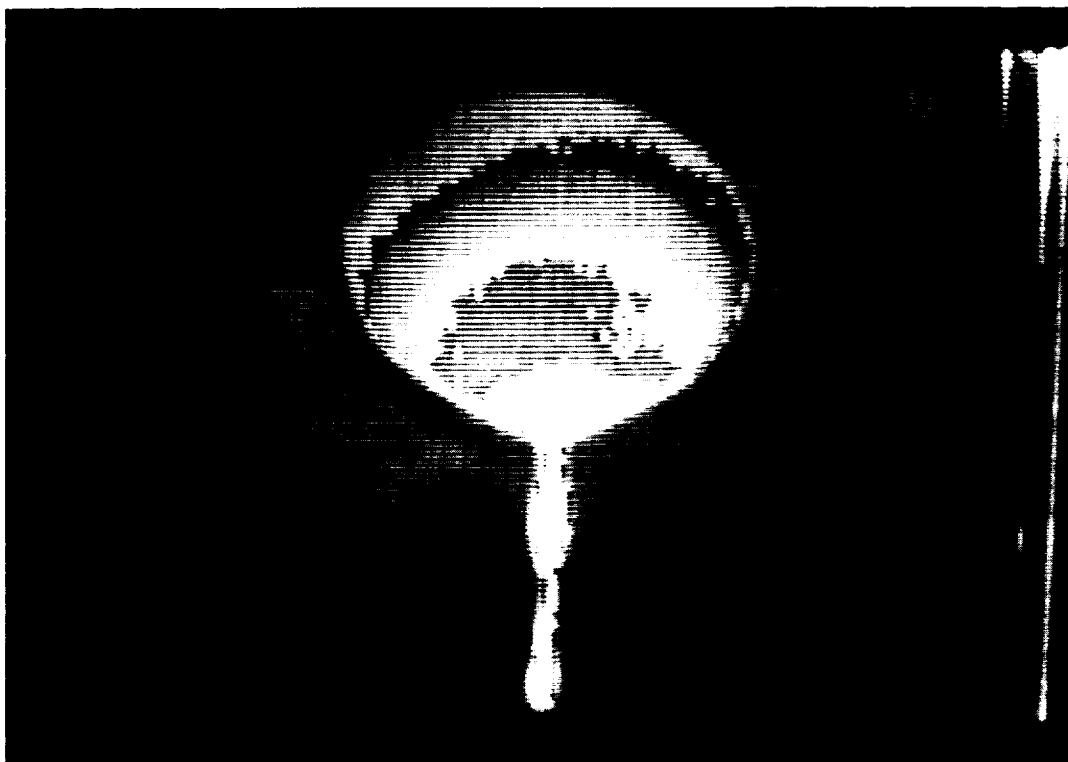


Figure 8.

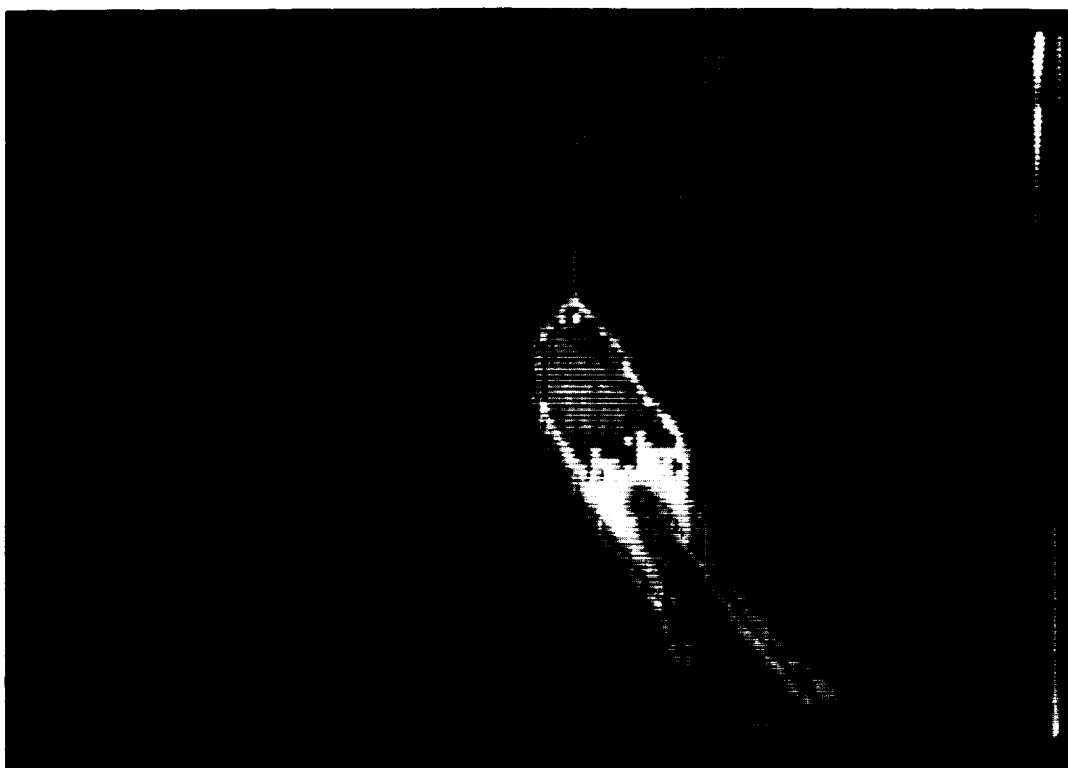


Figure 9.

ORIGINAL PAGE  
BLACK AND WHITE PHOTOGRAPH

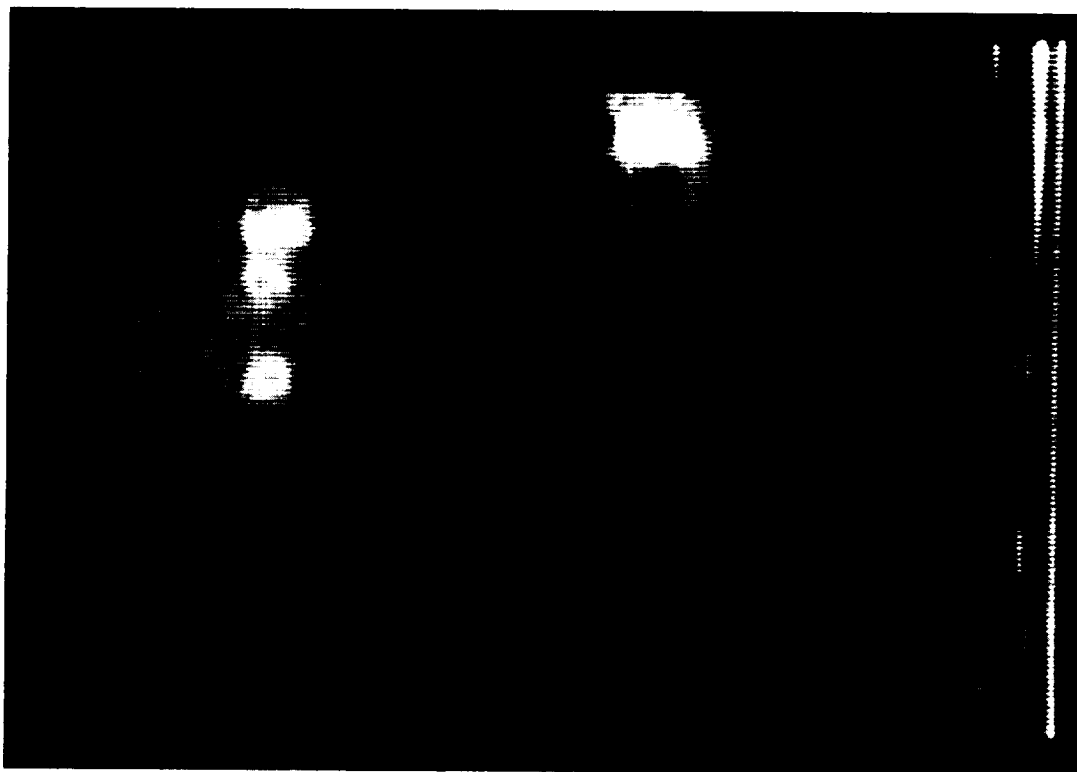


Figure 10.